İSTANBUL UNIVERSITY
CERRAHPAŞA

RESEARCH ARTICLE

Electrica 2021; 21(2): 216-224

A Novel Implementation of Deep-Learning Approach on Malaria Parasite Detection from Thin Blood Cell Images

Emrah Irmak

Department of Electrical and Electronics Engineering, Alanya Alaaddin Keykubat University, Antalya, Turkey

Cite this article as: E. Irmak, "A Novel Implementation of Deep-Learning Approach on Malaria Parasite Detection from Thin Blood Cell Images", Electrica, vol. 21, no. 2, pp. 216-224, May, 2021.

ABSTRACT

Malaria is known as an acute febrile disease caused by the bite of female Anopheles mosquitoes, and it manifests itself with symptoms such as headache, fever, chills, vomiting, and fatigue. The diagnosis of malaria is still based on manual identification of Plasmodium parasitized cells in microscopic examinations of blood cells known as parasite-based microscopy diagnostic testing. The accuracy of this manual diagnosis method is clearly affected by the level of microscopist's experience, which makes this diagnosis method susceptible to manual error and time consuming. Diagnoses of diseases made using deep-learning methods have had great repercussions in the medical world, especially in recent years; and this indicates that the diagnosis of malaria can also be achieved by deep-learning methods. On the basis of this fact, this paper presents a novel deep-learning-based malaria disease detection technique. A convolutional neural network (CNN) architecture, which has 20 weighted layers is designed and proposed to identify parasitized microscopic images from uninfected microscopic images. A total of 27,558 thin blood cell images were used to train and test the CNN model, and 95.28% overall accuracy was obtained. The experimental results on large clinical dataset show the effectiveness of the proposed deep-learning method for malaria disease detection.

Keywords: Convolutional neural network, deep learning, image classification, malaria disease detection

Corresponding Author:
Emrah Irmak

E-mail:
emrah.irmak@alanya.edu.tr

Received: January 12, 2021

Accepted: March 29, 2021

Available Online Date:
May 20, 2021

DOI: 10.5152/electrica.2020.21004

Introduction

Malaria is a contagious and deadly disease, which has been declared as an endemic in a lot of countries by the World Health Organization (WHO) [1]. It is caused by a virus known as *Plasmodium* parasite, which lives in the mosquito's body and is injected into affected person's blood once the mosquito bites the person [2]. In the 1000s of years of humanity's war with malaria, human beings have often been vulnerable to this disease. According to the reports of the WHO, the number of malarial cases and the number of people who have died from malaria in 2019 alone is 229 million and 409,000, respectively [3]. Another important statistic that stands out among these reports is that 67% (274,000) people who died from malaria disease were children under the age of five years, making it one of the leading causes of child mortality in the world. African countries, where approximately 94% of the number of malaria cases and deaths worldwide are seen, have been the disproportionate and indisputable center of this disease [3]. Figure 1 shows the annual number of deaths because of malarial disease reported by the Institute of Health Metrics and Evaluation (IHME) [4, 5]. According to this graph, the disease caused 670,000 deaths in 1990, peaked at 930,000 deaths in 2004, and caused 620,000 deaths in 2017.

Although there are therapeutic drugs for the treatment of the malaria, there is still not an effective vaccine against it, which makes it an active field of research. As malaria is a disease that can be transmitted from person to person, it is vital to diagnose it early and, thus, prevent its transmission. Making an accurate and successful diagnosis of malaria remains a task that only experienced microscopists can accomplish. As a matter of fact, microscopists examine billions of blood cell images by manually counting the parasites to be able to detect malaria every year throughout the world. However, an accurate and successful diagnosis of malaria cannot be a standard method common to all circles as it relies heavily on the experience and

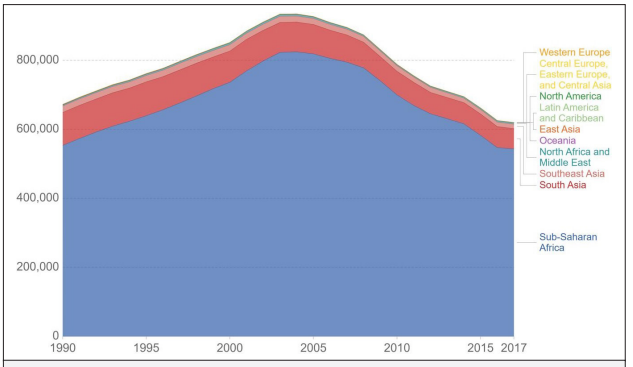

Figure 1. Annual number of deaths from malaria (Source: The Institute of Health Metrics and Evaluation)

skills of the microscopists. Besides, the insufficient number of microscopists constitutes a significant deficiency in combating malaria especially in developing countries. Computer-aided automated malaria parasite detection systems are superior to microscopic examinations. For example, deep-learning based malaria detection is more objective and quantitative compared with microscopic diagnosis, which is qualitative. These fully automatic methods are more reliable and standardized. Moreover, they allow clinicians to examine more patients, which make them faster than microscopic methods. Another advantage of deep-learning diagnosis methods over other manual diagnosis methods is that they are more economical such that they can reduce diagnostic costs.

Effective and successful studies of machine-learning methods in medical image processing and interpretation in the world have created a big trend for automatic diagnosis systems over the past decade. CNN has been one of the most commonly used automatic diagnosis technique among other deep-learning methods. CNN searches for and extracts the pathological features that appear different from the remaining tissues to be used as clinical decision-making tools [6, 7]. Despite highly promising findings of deep-learning methods for disease detection, just a few studies related to this subject have been reported. For instance, Rahman et al. [2] have proposed a deep CNN architecture consisting of a total of 19 weighted layers for malaria detection from microscopic images. They also investigated the effects of stain normalization, standardization, and data augmentation pre-processing techniques with several other pre-trained CNN models to evaluate the performance of transfer learning on malarial parasite detection. Another researcher group, Rajaraman et al. [8] have introduced an optimal deep neural ensemble consisting of custom and pre-trained CNN for malaria detection to improve robustness and generalization. Dong et al. [9] have shown that CNN-based classification of parasitized and uninfected thin blood microscopic images obtained a higher accuracy than that of kernel-based classification. Another research study [10] has demonstrated that shallow deep belief network could achieve a promising result in detecting the malarial parasite using peripheral smear images. Das et al. [11] have obtained an overall accuracy of 84% for detecting malaria using machine-learning approach from light microscopic images of peripheral smears. Ross et al. [12] have used an automated image processing method based on two-stage tree classifier and achieved an accuracy of 73% in diagnosis of malaria from thin blood smears. Researchers who are interested in more literature can investigate the publications [2, 13], which are rich reference sources in the field of machine-learning based malaria detection.

In this study, we aimed to detect malaria from red blood cell images using a fully automatic deep-learning model. A novel CNN architecture that consisted of 20 layers was prepared for malarial parasite detection. The proposed CNN model was trained on 22,046 thin blood images and tested on 5,512 thin blood images. The proposed method was validated using accuracy, area under the curve (AUC) of receiver operating characteristic (ROC) curve, specificity, sensitivity, and precision performance evaluation metrics. Experimental results on large microscopic data show the effectiveness of the proposed method. The rest of this study is organized as follows. The following section elaborates on the principles of CNN architecture. The reader can find explanation of each CNN layer and detailed mathematical formulas to create CNN layers in this section. Section 3 introduces the proposed CNN method. Section 4 includes experimental results, performance evaluation, and comparison of the proposed method with the state-of-art method. Finally, section 5 concludes the paper.

Basics of CNN Architecture

CNN layer

Input Layer

CNN's first layer is the input layer. In this layer, the data is fed raw to the neural network. The image is converted to a matrix of numeric expressions and then exported to the input layer. The data size in this layer in the digital environment is quite worthy of note for the success of the proposed model. Selecting a high input image size can result in high memory requirements, training time, and test time per image. It can also increase network success. Selecting a low input image size reduces memory requirements and reduces training time. However, the depth of the network to be installed decreases, and its performance can decrease. In performing image processing, a proper image size for input stage should be selected for network depth, hardware calculation cost, and network success.

Convolutional layer

This is the transformation layer that applies a specified filter over the whole input image. Because of this contribution of convolution filters, these filters are indispensable parts of layered architectures. Filter size may have 2×2, 3×3, 5×5, 7×7, etc., dimensions. The filters apply convolution process to the images coming from the previous layer and generate the output data. This filtering process results in a feature map (activation map). The feature map is the region where the features specific to each filter are discovered. The coefficients of these

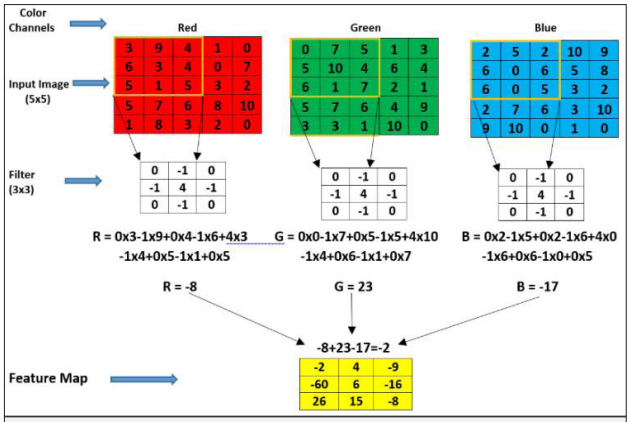

Figure 2. A 3 × 3 filter applied on an input image of size 5 × 5 × 3 in convolution layer of CNN

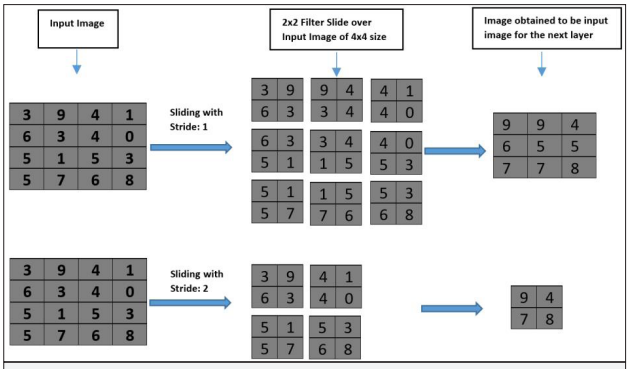

Figure 3. Implementation of max pooling with 2 × 2 filter in 4 × 4 input image

filters during training of CNNs vary with each learning iteration in the training set. The network, thus, determines which regions of the data are important to be able to determine the important features [14]. Applying a filter to the image and generating the feature map is shown in Figure 2.

In this layer, new feature sets are obtained by applying previously determined filters on the inputs. Each filter applied is represented by matrices of the specified size. Each filter applied to the input attempts to detect a different feature. Because very large filters can cause some features to be missed on the input, the dimensions of the filters are very important. The coefficients of the filters represent the weights in the artificial neural networks, and in each step, these filter coefficients are updated according to the error value to obtain new filters. Each filter circulates all pixels in sequence on the input. The input coefficients and the filter coefficients are multiplied as dot product, and this is done for each channel of the input image. As shown in the equation (1), feature maps are formed by multiplying the input matrix and weight matrices.

$$x_j^n = f\left(\sum_{i \in F_j} x_j^{n-1} k_{ij}^n + b_j^n\right) \quad (1)$$

where n is the number of layers in the convolutional layer, b is a bias, and:

i = the index of input neuron node

j = the index of output neuron node

f() = an activation function

F_j= upper level feature map

Rectified linear units layer (ReLU)

ReLU layer is a piecewise linear transfer function also known as the activation layer and is followed by the convolution layer. This layer transfers the positive inputs directly to the output but outputs zero for the negative ones. The network is linear at this stage because particular mathematical operations are performed in the layer used before this layer, that is, convolutional layer. ReLU layer is applied to bring this deep network into a non-linear structure, and this ensures that the network learns faster [14].

2.1.4. Pooling Layer

In the CNN architectures, the pooling layer comes after the ReLU layer and decreases the size of the input for the next convolution layer. This process is also known as "down sampling." The reduction in size as a result of this layer leads to information loss. A loss of this type is useful to the network in terms of two reasons. First of all, it produces less computational load to the following CNN layers. Second, it prevents the system from memorizing. Certain filters are defined in the pooling layer as in the convolution layer. These filters are applied on the image and process the maximum values of the pixels in the image (maximum pooling) or the average of the values (average pooling). As maximum pooling performs better than other pooling types, it is commonly preferred to other pooling types [14, 15]. Pooling layer performs the pooling process to all the images by the number of filters formed as a result of the convolutional layer [16]. Pooling is optional for the CNN, and some architectures do not use pooling layer. An example of how pooling is performed can be seen in Figure 3. Input image size is 4 × 4 and filter size is 2 × 2. The resulting image after sliding the input image with slide = 1 is 3 × 3 and with slide = 2 is 2 × 2 [14].

Fully connected layer

The fully connected layer together with the convolutional layer are the most important layers of CNN. The result of breaking down the image into features in the previous layers feeds into a fully connected layer, which determines the final classification. As the name implies, all neurons in the previous layers are connected with fully connected layer.

For instance, if the matrix size generated by the last layer in the CNN architecture is selected as 25 × 25 × 256 = 160,0000 × 1 and the matrix size in the fully connected layer is selected as 4,096 × 1, a total weighting matrix of 160,000 × 4,096 occurs. Therefore, this layer is called a fully connected layer. It forms the last layers of convolutional neural networks. In the layers up to the fully connected layer, feature extraction, size reduction and normalization operations are performed for the inputs. The

error is calculated according to the output. Weights are updated again according to the calculated error value, and this cycle continues until the desired convergence value is obtained or a certain number of steps are completed.

Softmax layer

Softmax layer is a normalized exponential function, which is used to bring all the predicted values between 0 and 1 using the equation (2).

$$y(z)_j = \frac{e^{z_j}}{\sum_{k=1}^{k} e^{z_k}} \quad (2)$$

where y(z) is the probability of any class, j indicates these classes, k is the total number of classes.

Classification layer

Classification layer comes after the fully connected and Softmax layers. Classification is done in this layer of deep-learning architectures. The number of classification objects is equal to the output value of this layer. For example, if the classification of 15 different objects is to be made, the classification layer output value must be 15. If the output value is selected as 4,096 in the fully connected layer, a weight matrix of 4,096 × 15 is obtained for the classification layer according to this output value [14]. In the classification, 15 different objects produce output at a certain value in the range 0–1. The output that produces close to 1 output is understood to be the object that the network predicts. The classifications layer uses cross-entropy loss to estimate the classification loss and provides the final predicted categorical label for each input image [17]. In this paper, cross-entropy loss [18] is calculated using equation (3).

$$H(p,q) = -\sum_{x}\left(p(x) * \log\left(q(x)\right)\right) \quad (3)$$

where *q(x)* is the estimate for true distribution , *p(x)* is the target labels vector, and *q* is the output vector from the SoftMax layer.

Proposed deep-learning method

Proposed CNN architecture

Deep-learning methods have been successfully used for the diagnosis of various diseases, especially over the past decade. One the most efficient class of deep-learning methods is obviously CNN. Therefore, malaria diagnosis is made using CNN technique in this study. Figure 4 shows the proposed CNN architecture. This CNN architecture includes 20 weighted layers. This is a novel CNN architecture designed for malaria disease detection. There are four convolution layers, four ReLU layers, four normalization layers, four max pooling layers, one fully connected layer, one Softmax layer, and one classification layer in this architecture. Thin blood images are re-sized to 44 × 44 × 3 and fed to the input layer. Convolution layers are applied to the input images to generate feature maps for training the network. ReLU layers are followed by convolution layers and used for activations. Max pooling layers come just after ReLU and normalization layers and are used for pooling process, which decreases the size of the input, thus reducing the computation burden. After that process, the fully connected layer with Softmax layer makes the final prediction regarding whether there is malaria or not. Classification layer has two neurons at output, each neuron for each class: "parasitized" or "uninfected." Hyper-parameters of the CNN model are as important as the architecture. In this proposed model, stochastic gradient descent momentum is used for minimizing the loss function and updating the parameters of the neural network. Three epochs are performed with mini-batch size equal to 64. The total number of iteration is 1,032 and the number of iterations per epoch is 344. The initial learning rate (ILR) and momentum (M) are tuned as 0.002 and 0.9, respectively.

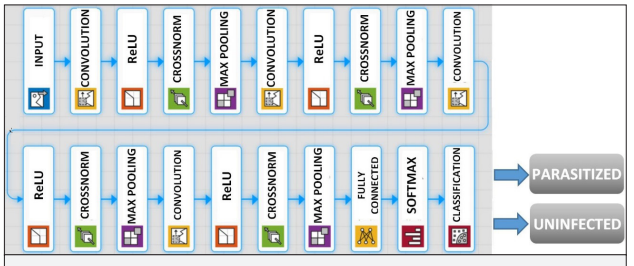

Figure 4. The proposed CNN architecture

Performance assessment

It is necessary to evaluate the success of the classification task after the classification task is performed. The performance of the classification tasks can be evaluated using various performance evaluation metrics. For example, confusion matrix is the main source of these metrics. Confusion matrix is known as a specific two-dimensional table with "actual" and "predicted" labels. The actual label is for instances in an actual class, whereas the predicted label is the system output predictions. Therefore, the confusion matrix, being an error matrix, provides visually very important information for the performance evaluation. In this study, the performance of the proposed CNN method is evaluated using accuracy, AUC, sensitivity, specificity, and precision performance evaluation metrics, which are derived from confusion matrix. Equations (4) through (7) show the corresponding formulas that belong to these metrics, respectively. True positive (TP) is the number of system's positive predictions, which are actually positive. True negative (TN) is the number of system's negative predictions, which are actually negative. False positive (FP) is the number of system's positive predictions, which are actually negative. False negative (FN) is the number of system's negative predictions, which are actually positive.

$$\text{Accuracy} = \frac{TP+TN}{TP+TN+FP+FN} \quad (4)$$

$$\text{Specificity} = \frac{TN}{TN+FP} \quad (5)$$

$$\text{Sensitivity} = \frac{TP}{TP+FN} \quad (6)$$

$$\text{Precision} = \frac{TP}{TP+FP} \quad (7)$$

Results and Discussion

Dataset

This study is implemented on the Giemsa-stained thin blood (red blood cell) images from the dataset created by National Institute of Health (NIH) [19]. These images were collected from 50 healthy patients and 150 patients infected with *Plasmodium falciparum*. The dataset contains a total of 27,558 red blood cell images; 13,779 infected and 13,779 uninfected. An expert slider reader pathologist manually annotated the images. Some sample images from this dataset are demonstrated in Figure 5. The differences in colors are owing to the different stains during image acquisition. Malaria infected images have numerous forms of parasites.

Experiment platform and time consumption

The experiments of this study were performed on an NVIDIA GeForce GTX-850M platform that had Intel Core i7 5400 GPU, 2.60 GHz, 16.0 GB RAM, whereas the software platform consisted of Windows 10 (64-bit) operating system software platform using MATLAB 2019a version. Thirty four minutes elapsed throughout the training of the proposed CNN model.

Experimental results

The dataset was divided into training (60%), validation (20%), and test (20%) sets; therefore, 16,534 images were stored for training, 5,512 images for validation, and 5,512 images for testing purposes. For dataset training and testing, the five-fold cross-validation procedure was used. Five independent iterations were performed. One of the folds was used as the test set, and the remaining were used as the training set. This process was repeated until each unique fold had been used as the test set. The CNN model performs the learning process in a hierarchical structure, consisting of multiple trainable layers, one after the other. After the input data are received, the training process is carried out by making layer-by-layer transactions on CNN. The first convolution layer in the CNN model generally learns very basic structures (features), such as colors and edges. More details and complicated features are learned in deeper convolution layer. The features that the CNN learns after the training may be understood by visualizing the activations of the convolution layers. Figures 6 (a) and 6 (b) show the activations of the first and second convolution layers, respectively, after a parasitized red blood cell microscopic image is fed into the CNN model. It can be seen in Figure 6 (a) that color and edges that are simple features are learned in this early layer, whereas in Figure 6 (b) parasite structures that are more complicated features are learned in the deeper convolution (second) layer. As a consequence, one can discover the features that are learned by the network using this visualization of the activations.

Once the classification task is performed, the performance of the implementation is evaluated using confusion matrix. Confusion matrix is shown in Figure 7. Vertical axis in the confusion matrix represents the system's output predictions (output class), whereas the horizontal axis represents ground truth

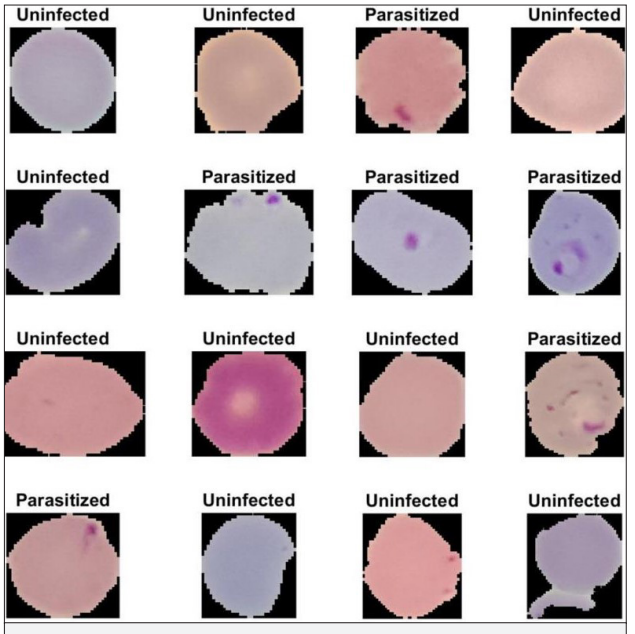

Figure 5. Samples of thin blood cell images drawn from dataset that contains parasitized and uninfected images

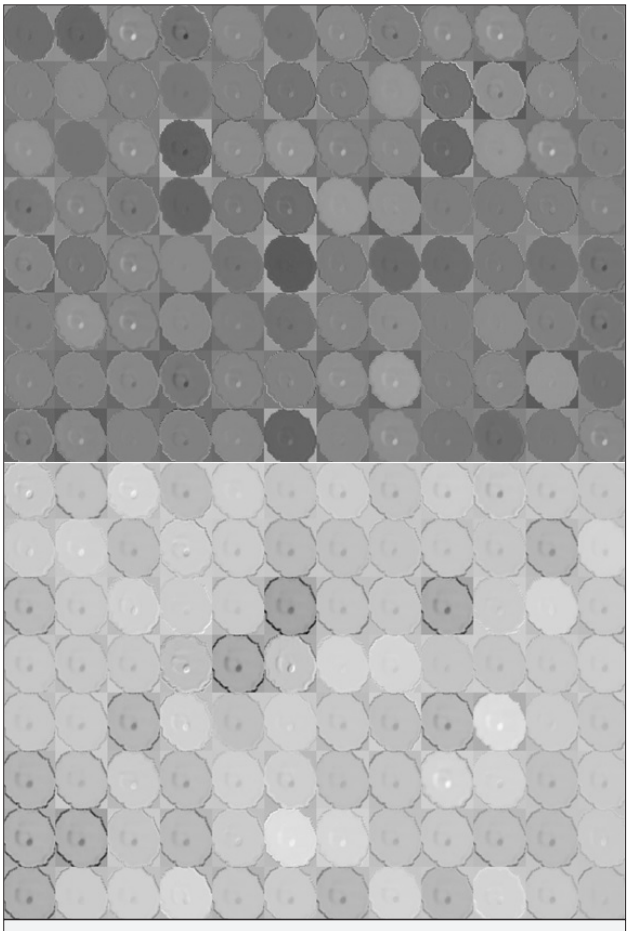

Figure 6. a, b. Activations of first (a) and second convolutional layer (b)

(target class) labels. Performance evaluation of the proposed method is assessed using accuracy, AUC, sensitivity, specificity, and precision whose formulae are given in equations (4–7). Detailed results of the performance evaluation metrics are shown in Table 1. A total of 2,756 parasitized and 2,756 uninfected microscopic red blood cell images were used for testing the proposed CNN model, which was designed to diagnose malaria.

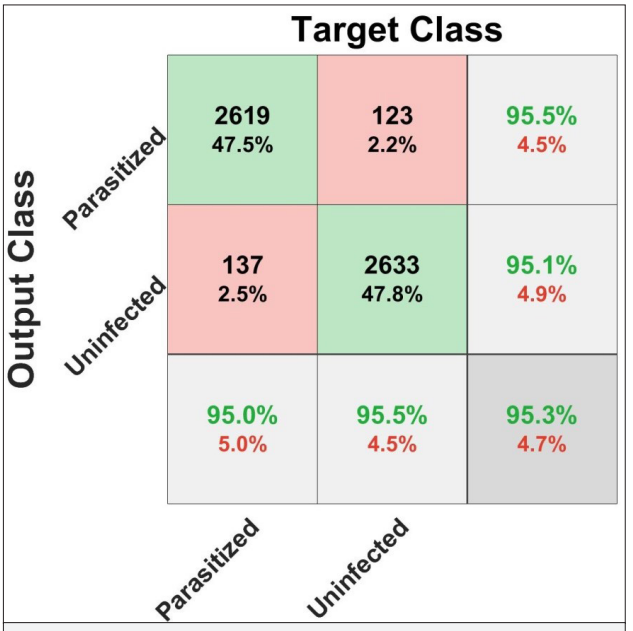

Figure 7. Confusion matrix

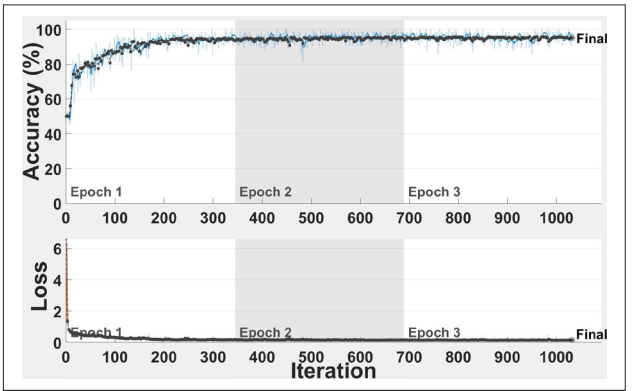

Figure 8. Accuracy and loss plot

Table 1 demonstrates that the proposed method can detect malaria with an accuracy of 95.28%, sensitivity of 0.950, specificity of 0.955, and precision of 0.955.

Accuracy and loss plots are demonstrated in Figure 8. As the figure shows clearly, 95.28% accuracy is achieved after 1,032 iterations. Figure 9 is the ROC curve of the classification task. Y-axis of ROC curve is true positive rate (TPR) and X-axis is false positive rate (FPR). This ROC curve figure shows that AUC value which is a measure of the entire two-dimensional area underneath the entire ROC curve is found to be 0.9886.

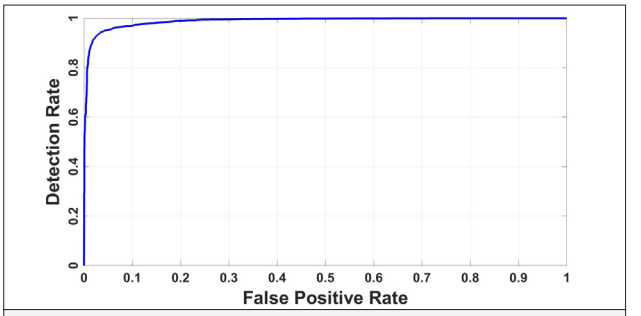

Figure 9. Receiver operating characteristic curve

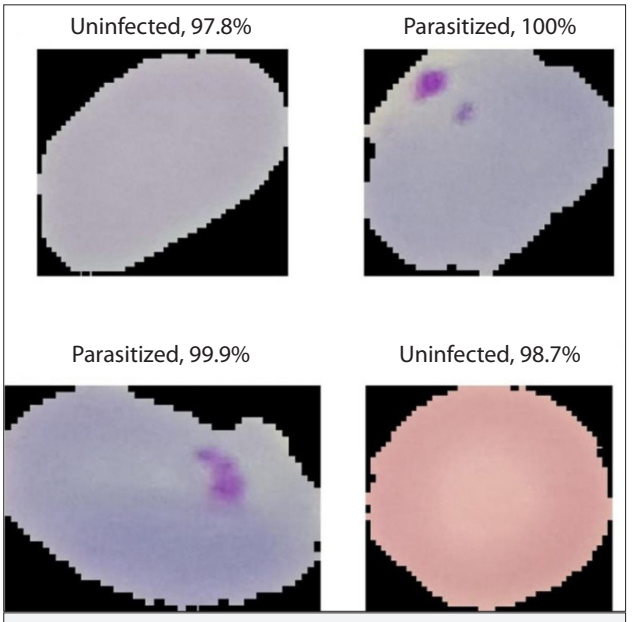

Figure 10. Four input test images results

Table 1. Accuracy metrics in terms of TP, TN, FP, FN, Accuracy, Specificity, Sensitivity, and Precision

Metrics

Architecture	Classes	TP	TN	FP	FN	Accuracy	Specificity	Sensitivity	Precision	Total
Proposed CNN Architecture	Parasitized	2619	2633	123	137	95.28%	0.955	0.950	0.955	2756
	Uninfected	2633	2619	137	123	95.28%	0.950	0.955	0.951	2756

TP: True Positive; TN: True Negative; FP: False Positive; FN: False negative; CNN: Convolutional Neural Network

Figure 10 shows the classification results of the proposed CNN model, which is designed to classify input images as parasitized (malaria) and uninfected (healthy). The model does not only predict malaria but also gives the prediction probability of the output class. Of the four test images, two input images are predicted as parasitized with 100% and 99.9% probabilities, respectively. The remaining two input test images are classified as uninfected with 97.8% and 98.7% probabilities, respectively.

Class activation map (CAM) tool is used to understand the decision making of the proposed CNN. Figure 11a is a parasitized input image, whereas Figure 11c is the uninfected input image. Figure 11b is the CAM output of a parasitized cell image, whereas the Figure 11d is the output of an uninfected image. Activation in the CAM outputs show that the CNN model has learned task-specific features.

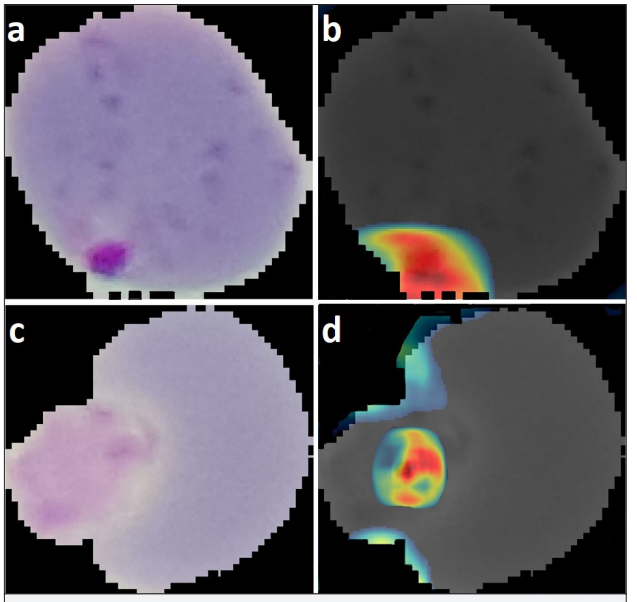

Figure 11. a-d. Class activation map (CAM) visualization results: (a) Parasitized input image, (b) CAM output of parasitized input image, (c) Uninfected input image, (d) CAM output of uninfected input image

Comparison with state-of-the-art methods

This section is devoted to the comparison of the proposed method with state-of-the-art methods. Dong et al. [9] have shown that CNN-based classification of parasitized and uninfected thin blood microscopic images could obtain an accuracy of 95% using three well-known pre-trained CNN architecture, such as LeNet, AlexNet, and GoogleNet. The total number of images was 2,565, which included 1,034 parasitized and 1,531 uninfected images. Bibin et al. [10] have proposed an automated decision support system based on deep learning to detect the malarial parasite from peripheral blood smear images. They used 4,100 microscopic images and obtained 96.21% accuracy. Das et al. [11] have used the machine-learning approach to discriminate between healthy and malarial parasite infected images with 84% accuracy. Ross et al. [12] have presented an automatic image processing technique that consists of two-stage tree classifier to identify malarial parasites present in thin blood smears with an overall accuracy of 73%. Vijayalakshmi et al. [20] have proposed transfer-learning approach based on visual geometry group (VGG) network and support vector machine (SVM) to identify parasitized malarial blood cell images. They achieved 93.13% classification accuracy using 1,530 images. Narayanan et al. [21] have proposed image pre-processing approach with a fast CNN model for malaria parasite detection. They achieved 96.7% overall accuracy using the same dataset used in the proposed study. In another study by Narayanan et al. [22], they have used GoogleNet and ResNet for the detection of *Plasmodium* on cell images captured using digital microscopy. They obtained 96.6% accuracy using ResNet and 96.5% accuracy using GoogleNet with pre-processing approaches. The

Table 2. Detailed comparison of the proposed method with state-of-the-art methods

Model	Overall accuracy	Number of images	Method	Publication year
Ross et al. [12]	73.00%	15	Decision tree	2006
Das et al. [11]	84.00%	27,558	Bayesian classifier and SVM	2013
Mandal et al. [23]	88.77%	37	Segmentation-Normalized cuts	2010
Le et al. [24]	92.69%	200	Semi-automatic image processing	2008
Vijayalakshmi et al. [20]	93.13%	27,558	Pre-trained CNNs	2019
Dong et al. [9]	95.00%	2,565	Pre-trained CNNs	2017
Bibin et al. [10]	96.21%	4,100	Deep Belief Network	2017
Narayanan et al. [21]	96.7%	27,558	Custom CNN	2019
Narayanan et al. [22]	96.6%	27,558	Pre-trained CNNs	2019
Proposed Method	95.28%	27,558	A Novel CNN	2021

proposed CNN architecture in this paper achieved an overall accuracy of 95.3%, trained and tested on 27,558 thin blood images. This experimental result on large microscopic image dataset shows the effectiveness of the proposed method considering the literature. Table 2 shows a detailed comparison of the results found using the proposed method with the results of the state-of-the-art methods.

Conclusion

One of the hurdles to successful mortality reduction has been inadequate diagnosis of malaria. However, the most effective progress in the prevention of the disease is early diagnosis, which enables interrupting its transmission. In this study, we presented a novel and fully automatic method using deep convolutional neural networks for detection of malaria from red blood cell images. A novel CNN architecture was designed and proposed for malarial disease diagnosis using a large publicly available dataset. Detection of malaria was achieved with a high accuracy of 95.28%. Experimental results on a large clinical dataset show the effectiveness of the proposed CNN architecture. It is believed that owing to its simplicity, the model proposed in this study can be readily used in practice to help physicians diagnose malaria accurately. This fully automatic deep-learning method has the potential to allow clinicians to examine more patients, which makes it faster than microscopic malaria examination methods [9-12, 20-24].

Peer-review: Externally peer-reviewed.

Conflict of Interest: The author have no conflicts of interest to declare.

Financial Disclosure: The author declared that this study has received no financial support.

References

1. "World Health Organization." https://www.who.int (accessed Dec. 21, 2020).
2. A. Rahman, H. Zunair, M. S. Rahman, J. Q. Yuki, S. Biswas, A. Alam, N. B. Alam, M. R. C. Mahdy, "Improving malaria parasite detection from red blood cell using deep convolutional neural networks," arXiv, pp. 1-33, Jul. 2019.
3. Global Malaria Program, "World malaria report 2019," 2020. [Online]. Available: https://www.who.int/publications/i/item/9789241565721.
4. "Our world in data." https://ourworldindata.org/malaria (accessed Jan. 03, 2021).
5. M. Roser, R. Hannah, "Malaria," Our World in Data, 2013. https://ourworldindata.org/malaria (accessed Jan. 04, 2021).
6. E. Irmak, "Implementation of convolutional neural network approach for COVID-19 disease detection," Physiological Genomics, vol. 52, no. 12, pp. 590-601, Dec. 2020. [Crossref]
7. E. Irmak, "A novel deep convolutional neural network model for COVID-19 disease detection," Medical Technologies National Conference (TIPTEKNO), 2020, no. 11, pp. 39-42. [Crossref]
8. S. Rajaraman, S. Jaeger, S. K. Antani, "Performance evaluation of deep neural ensembles toward malaria parasite detection in thin-blood smear images," PeerJ, vol. 7, p. e6977, May 2019. [Crossref]
9. Y. Dong, Z. Jiang, H. Shen, W. D. Pan, L. A. Williams, V. V. B. Reddy, W. H. Benjamin, A. W. Bryan, "Evaluations of deep convolutional neural networks for automatic identification of malaria infected cells," IEEE EMBS International Conference on Biomedical & Health Informatics (BHI), pp. 101-104, 2017. [Crossref]
10. D. Bibin, M. S. Nair, P. Punitha, "Malaria parasite detection from peripheral blood smear images using deep belief networks," IEEE Access, vol. 5, pp. 9099-9108, May 2017. [Crossref]
11. D. K. Das, M. Ghosh, M. Pal, A. K. Maiti, C. Chakraborty, "Machine learning approach for automated screening of malaria parasite using light microscopic images," Micron, vol. 45, pp. 97-106, Feb. 2013. [Crossref]
12. N. E. Ross, C. J. Pritchard, D. M. Rubin, A. G. Dusé, "Automated image processing method for the diagnosis and classification of malaria on thin blood smears.," Medical & Biological Engineering & Computing, vol. 44, no. 5, pp. 427-436, May 2006. [Crossref]
13. M. Poostchi, K. Silamut, R. J. Maude, S. Jaeger, G. Thoma, "Image analysis and machine learning for detecting malaria,"Translational Research, vol. 194, pp. 36-55, Apr. 2018.[Crossref]
14. O. Inik E. Ulker, "Deep learning and deep learning models used in image analysis," Gaziosmanpasa Journal of Scientific Research, vol. 6, no. 3, pp. 85-104, 2017.
15. Q. Zhao, S. Lyu, B. Zhang, W. Feng, "Multiactivation Pooling Method in Convolutional Neural Networks for Image Recognition," Wireless Communications and Mobile Computing, vol. 2018, pp. 1-16, 2018. [Crossref]
16. Ş. Okul, D. Aksu, M. A. Aydin, "Applications of Deep Learning and Big Data Technologies," 16th Int. Multi-Conference Syst. Signals Devices, SSD 2019, pp. 550-553, 2019, doi: [Crossref]
17. H. H. Sultan, N. M. Salem, W. Al-Atabany, "Multi-Classification of Brain Tumor Images Using Deep Neural Network," IEEE Access, vol. 7, no. May, pp. 69215-69225, 2019. [Crossref]
18. Y. Zhou, X. Wang, M. Zhang, J. Zhu, R. Zheng, Q. Wu, "MPCE: A Maximum Probability Based Cross Entropy Loss Function for Neural Network Classification," IEEE Access, vol. 7, pp. 146331-146341, 2019. [Crossref]
19. "Malaria cell images dataset, National Institute of Health (NIH)." https://ceb.nlm.nih.gov/repositories/malaria-datasets/ (accessed Dec. 21, 2020).
20. A. Vijayalakshmi, B. Rajesh Kanna, "Deep learning approach to detect malaria from microscopic images," Multimedia Tools and Applications, vol. 79, no. 21-22, pp. 15297-15317, 2020. [Crossref]
21. B. N. Narayanan, R. Ali, R. C. Hardie, "Performance analysis of machine learning and deep learning architectures for malaria detection on cell images," in Proceedings of SPIE : Applications of Machine Learning, International Society for Optics and Photonics, vol. 11139, p. 111390W, Sep. 2019. [Crossref]
22. B. N. Narayanan, S. M. S. De, H. R. C., Kueterman; Nathan K., R. Ali, "Understanding Deep Neural Network Predictions for Medical Imaging Applications," arXiv, 2019.
23. S. Mandal, A. Kumar, J. Chatterjee, M. Manjunatha, A. K. Ray, "Segmentation of blood smear images using normalized cuts for detection of malarial parasites," in Proceedings of the 2010 Annual IEEE India Conference: Green Energy, Computing and Communication, INDICON, no. Jan 2010, doi: 10.1109/INDCON.2010.5712739. [Crossref]
24. M. T. Le, T. R. Bretschneider, C. Kuss, P. R. Preiser, "A novel semi-automatic image processing approach to determine Plasmodium falciparum parasitemia in Giemsa-stained thin blood smears," BMC Molecular and Cell Biology, vol. 9, no. 15, 2008. [Crossref]

Emrah Irmak was born in 1988 in Mardin, Turkey. He received his B.Sc. and M.Sc. degrees in Electrical and Electronics Engineering from Gaziantep University, Gaziantep, Turkey, in 2012 and 2014, respectively. He received his PhD in Electrical and Electronics Engineering from Karabuk University, Karabuk, Turkey in 2018. He worked as a research assistant in the Biomedical Engineering Department in Karabuk University between 2012 and 2019. He is currently an assistant professor in the Electrical and Electronics Engineering Department in Alanya Alaaddin Keykubat University, Antalya, Turkey. His research interests include medical image processing, signal processing, and deep learning.